Small angle x-ray scattering for sub-100 nm pattern characterization

Ronald L. Jones, Tengjiao Hu, Eric K. Lin, and Wen-Li Wu[a)]
NIST Polymers Division, Gaithersburg, Maryland 20899-8541

Rainer Kolb
ExxonMobil Research and Engineering Company, Annandale, New Jersey 08801

Diego M. Casa
CMC-CAT, Advanced Photon Source, Argonne National Laboratory, Argonne, Illinois 60439

Patrick J. Bolton and George G. Barclay
Shipley Company, Incorporated, Marlborough, Massachusetts 01752

(Received 21 March 2003; accepted 3 September 2003)

Characterization of sub-100 nm photolithographic patterns with nanometer scale resolution is demonstrated using small angle x-ray scattering. The transmission scattering geometry employed potentially enables high throughput measurements for future technology nodes of the semiconductor industry, organic and inorganic nanoscale devices, and three-dimensional structures. The method is demonstrated through the characterization of a series of polymer photoresist gratings using a synchrotron x-ray source. Quantities, such as periodicity and line width, are extracted using minimal modeling. Additional quantities and the potential of a laboratory-based x-ray system are briefly discussed. © *2003 American Institute of Physics.* [DOI: 10.1063/1.1622793]

The mass production of semiconductor devices possessing sub-100 nm features requires the development of metrologies capable of rapid measurement of pattern shape and size with subnanometer precision.[1] To serve the broader community of micro- and nanoscale devices, a technique should possess equivalent capabilities for a range of materials including organic, inorganic, conducting, insulating, and semiconducting. The technique must allow routine measurement of test patterns used to evaluate photoresists and process quality, typically on the order of 50×50 μm. Current measurement techniques, including scanning electron microscopy (SEM), electrical critical dimension, and atomic force microscopy all face serious challenges in their application at the current 100 nm regime and beyond.[2,3] Light scatterometry has recently emerged as a significant tool in both development and process characterization,[4] however, the sensitivity of large wavelength probes ($\sim$ 400 nm) is reduced as the dimensions of dense structures continue to shrink. We report initial results from measurements of a series of photoresist gratings, using transmission small angle x-ray scattering (SAXS) measurements (see Fig. 1). The results demonstrate a capability of determining feature shape and quality with nanometer-scale resolution for patterns produced using current photolithographic methods. This technique is readily extended into future technology nodes.

The advantages of subnanometer wavelength scattering in submicron patterns have been demonstrated through a variety of scattering techniques.[5–11] However, these demonstrations have often lacked a general applicability to actual industrial test structures. These limitations are overcome using a transmission geometry with a pinhole geometry to provide an appropriate beam spot size $<50\times50$ μm. The resulting data are then interpreted with established diffraction theory. The relatively small interaction between x rays and most materials allows a general application of the technique to a wide range of materials, including inorganic, such as oxide or metallic, and organic materials such as in photoresists. The lower relative electron density of photoresists is an appropriate test of SAXS capabilities since other materials including copper and silica have a higher electron density which results in higher diffracted intensity. Cases with copper line patterns will be presented in future articles.

As a demonstration of this technique, we provide initial results from measurements of photoresist gratings possessing a critical dimension (CD)$\approx$180 nm. Photoresist gratings, shown in Fig. 2, are often used to evaluate photoresist quality and imaging conditions, and therefore serve as an appropriate sample for these initial experiments. The three gratings are composed of different photoresist formulations, where

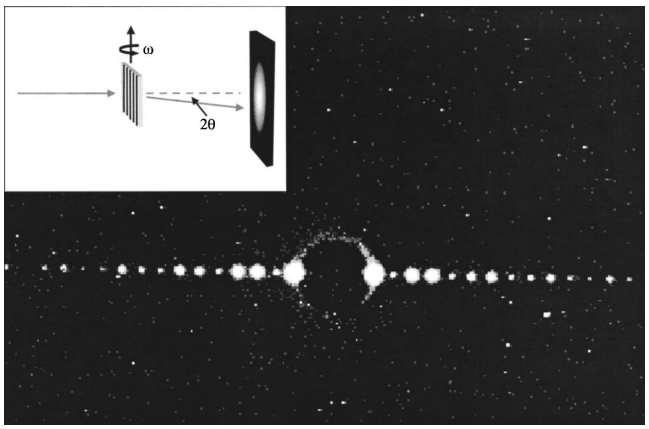

FIG. 1. Image of SAXS intensity on the two-dimensional detector, where the beam size is approximately 40×40 μm. Also shown in the inset is a schematic of the scattering geometry, showing the scattering angle, 2θ, and the sample rotation axis, ω.

[a)]Author to whom correspondence should be addressed; electronic mail: wenli@nist.gov

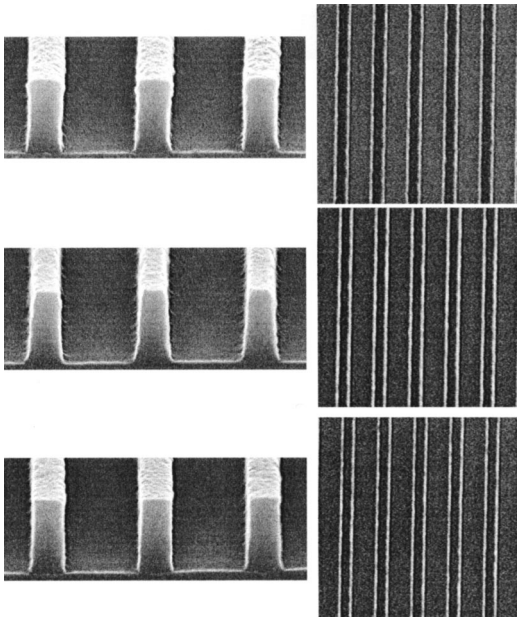

FIG. 2. SEM images of photoresist gratings A (top), B (middle), and C (bottom). Shown are the gratings in cross section (left-hand side) and top down (right-hand side) views.

each sample is imaged with the same mask at optimal conditions for the resist. SAXS measurements were performed at the 9ID beamline of the Advanced Photon Source (Argonne National Laboratory) using a two-dimensional charge coupled device detector 543 cm from the sample. Beam optics included a monochromator, two focusing mirrors along normal axes, and two beam definition slits before the sample. The intensity, I, is recorded as a function of the scattering vector, q [$=4\pi\sin(\theta)/\lambda$, where 2θ is the scattering angle measured relative to the direct beam and λ is the wavelength], as shown schematically in Fig. 1.

The choice of wavelength is key to the application of transmission SAXS to patterns on a silicon wafer. As shown in Fig. 1, interaction with the patterns, typically on the order of 500 nm in height, occurs after passing through nearly a millimeter of substrate material. A wavelength of 0.095 nm is chosen to reduce substrate absorption while retaining acceptable resolution. At this wavelength, the measurement time of a single sample is on the order of seconds. In Fig. 1, diffraction spots from an array of photoresist lines are observed beyond the 14th order of diffraction (the first order is blocked by the beamstop). Initial measurements presented here (in Figs. 3 and 4) employ a beam spot size of $100\times100\ \mu$m, however later refinements of the optical elements produced a beam spot size more amenable to test structure dimensions with a size of $40\times40\ \mu$m (shown in Fig. 1). While a smaller beam size is more convenient, the results did not alter the precision or accuracy of the results from the larger beam size.

Given in Fig. 1, a photoresist grating produces a one-dimensional series of diffraction spots. The intensities along the diffraction axis from each sample are plotted as a function of q in Fig. 3. The subtle differences observed in the SEM micrographs are apparent as variations in relative peak intensities in Fig. 3 (for example, see the 12th-order peak). For a given rotation angle, ω, the diffraction peak spacing, Δq, is inversely proportional to the repeat period, L, projected on the detector plane, where $\Delta q=2\pi/(L\cos\omega)$. A linear fit of the peak intensity position as a function of peak order provides the periods for each sample as $(L\cos\omega)=[553\pm5.4]$ nm, $[550\pm6.4]$ nm, and $[543\pm4.5]$ nm for the A, B, and C samples, respectively.[12] For a system with precise sample positioning, the angle ω can be known to within 0.001°. In the absence of a sample positioning device of high precision, we quote only the uncertainty in the projected repeat distance. We believe the uncertainty in ω quoted here is primarily responsible for the large deviation in the reported values of $L\cos\omega$.

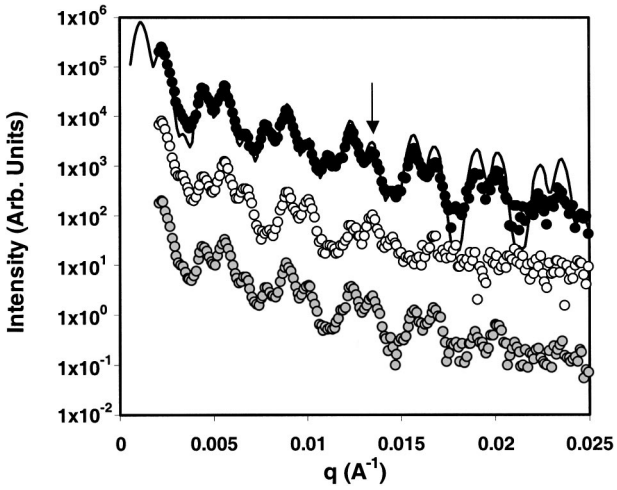

FIG. 3. SAXS intensity as a function of q for samples A (top), B (middle), and C (bottom). Intensities are arbitrarily offset for clarity. For sample A, a fit of the product $|S(q)*P(q)|^2$ is shown. The arrow indicates the 12th order of diffraction.

The average feature width is obtained from the relative intensities of the peaks. The intensities are fit using the form $I_{\text{peak}}(q)=A*|P(q)|^2$, where A is an arbitrary constant and $P(q)$ is the form factor of a line with rectangular cross section [$=\sin(qd)/q$, where d is the width of the line]. The use of $P(q)$ is general for obtaining an average feature width. If the features were, for instance, contact holes with cylindrical

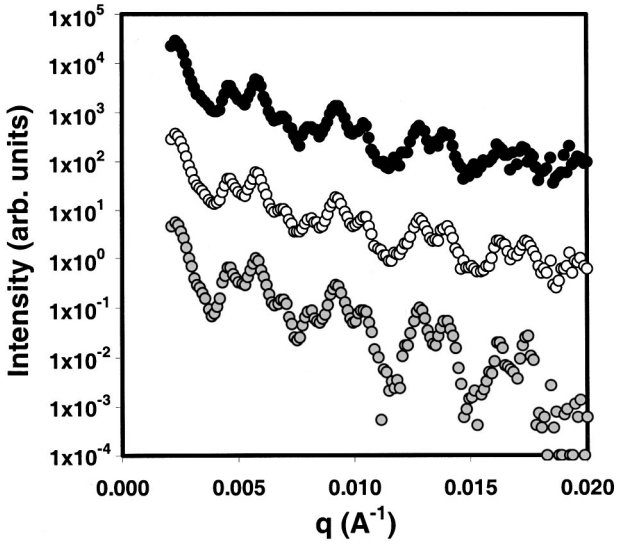

FIG. 4. SAXS intensity of sample C measured at sample rotations of 0° (top), 3° (middle), and 5° (bottom) of rotation. Intensities are shifted for clarity.

symmetry, this analysis would provide the average radius projected along the diffraction axis. A fit of $I_{peak}(q)$ for each of the samples yields $d=[171\pm3.6]$ nm, $[159\pm4.8]$ nm, and $[167\pm2.7]$ nm for the A, B, and C samples, respectively. Because there is a conservation relation between pitch, linewidth, and the width of the spaces, the form factor $P(q)$ has two equivalent solutions representing the linewidths and space widths. For the 1:2 spacing measured here, these two length scales are sufficiently separated and the assignment is trivial. For the case of 1:1 spacing where the differences in the two lengths are on the order of nanometers, assigning a value of d based on $P(q)$ alone becomes problematic. For this case, the ability to distinguish between two phases relies on absolute intensity. Here, the absolute intensity will change as a function of the total amount of photoresist. Future studies will be required to determine the limits of precision of this type of analysis.

Fitting $P(q)$ using a trapezoid rather than a rectangle ideally yields an average sidewall angle. Using this formalism, the effective sidewall angles of the three samples are estimated at 88.2°, 87.9°, and 88.5° for samples A, B, and C, respectively. We note that while these results appear consistent with the SEM cross-sectional images of Fig. 2, these numbers may be affected by other defects not included in this simple model including sidewall roughness and should therefore be considered only qualitatively. Additional information on line shape is ideally obtained by measurement along varying angles of sample rotation. Using this method with SAXS, an average sidewall angle has been previously demonstrated.[13] The measurement of a feature can be approximated as a projection of the density of the material. A footed feature will project a different distribution of electron density than an undercut feature at a nonzero angle ω. At sufficient large ω, the distance H between the center of mass of the feature to the silicon substrate can be determined. A comparison between the measured value of H and the sample height will help to differentiate a footed feature versus an undercut one. For a footed feature its H is less than half of the sample height and the opposite is true for an undercut one. The limits measurable by this technique, however, will rely on more complex models and are not determined by the current study. In Fig. 4, data from sample C as a function of ω show an expected variation of projected repeat distance, but do not exhibit large changes in the form factor $P(q)$. The invariance of $P(q)$ suggests a relatively vertical sidewall.[13] Continued efforts are required to develop more precise models distinguishing sidewall defects.

The application of this technique to sub-100 nm dimensions will result in the same form of data as presented in this work, however the q range will now be expanded. The highly monochromatic beam ($\Delta\lambda/\lambda\approx3\times10^{-5}$) used here provides a nearly fixed resolution for even a relatively large q range. As a result, data analysis and structural determination will not change for future technology nodes.

The prospect of conducting this type of CD measurement using laboratory x-ray equipment is of interest. The issue is whether the scattering peak intensity from features of 1 μm in height is sufficient to be detected with a laboratory unit. To address this issue, the peak intensity of samples, similar to that reported here, is reduced to absolute intensity using a polyethylene blank with precalibrated x-ray scattering cross section as the secondary standard. The peak intensity ranged from 10^7 cm^{-1} to 10^5 cm^{-1} over the q range [0 to 0.025] Å^{-1}—the same range as shown in Fig. 3. Scattering intensity of this magnitude is readily observable with a laboratory unit equipped with a sub-Angstrom x-ray source.

In conclusion, we have demonstrated the potential of SAXS as a measurement tool for pattern characterization in sub-100 nm lithographic processing. The technique was demonstrated using a series of photoresist test gratings characteristic of scatterometry test patterns already employed industrially. The low contrast of organic patterns suggests a ready application of the technique to inorganic systems such as is found in copper interconnects. The technique currently provides resolution on the order of 3–4 nm, extendible to subnanometer levels with finer adjustments of x-ray optics or increased pattern quality.

This work was funded in part by the DARPA Advanced Lithography Program under Contract No. N66001-00-C-8083. Additional funding was provided by the NIST Office of Microelectronic Programs. The Advanced Photon Source and one of the authors (D.M.C.) are supported by the U.S. Department of Energy under Contract No. W-31-109-ENG-38. Another author (R.L.J.) is supported by a NIST National Research Council postdoctoral fellowship.

[1] *International Technology Roadmap for Semiconductors*, 2001 Edition, SIA, 2001.
[2] J. Villarubia, R. Dixson, S. Jones, J. R. Lowney, M. T. Postek, R. A. Allen, and M. W. Cresswell, Proc. SPIE **3677**, 587 (1999).
[3] C. Nelson, S. C. Palmateer, A. R. Forte, and T. M. Lyszczarz, J. Vac. Sci. Technol. B **17**, 2488 (1999).
[4] C. J. Raymond, M. R. Murnane, S. L. Prins, S. Sohail, H. Naqvi, and J. R. McNeil, J. Vac. Sci. Technol. B **15**, 361 (1997).
[5] M. Gailhanou, T. Baumbach, U. Marti, P. C. Silva, F. K. Reinhart, and M. Ilegems, Appl. Phys. Lett. **62**, 1623 (1993).
[6] Q. Shen, C. C. Umbach, B. Weselak, and J. M. Blakely, Phys. Rev. B **48**, 17967 (1993).
[7] P. van der Sluis, J. J. M. Binsma, and T. van Dongen, Appl. Phys. Lett. **62**, 3186 (1993).
[8] M. Tolan, W. Press, F. Brinkop, and J. P. Kotthaus, Phys. Rev. B **51**, 2239 (1995).
[9] G. T. Baumbach, D. Lubbert, U. Pietsch, N. Darowski, L. Leprince, A. Talneau, and J. Schneck, Physica B **248**, 343 (1998).
[10] V. Holy, J. Stangl, G. Springholz, M. Pinczolits, and G. Bauer, J. Phys. D **34**, A1 (2001).
[11] E. K. Lin, R. L. Jones, W.-L. Wu, J. G. Barker, P. J. Boulton, and G. G. Barclay, Proc. SPIE **4689**, 541 (2002).
[12] The data in this manuscript, in the figures, and in the tables are presented along with the standard uncertainty (±) involved in the measurement, where the uncertainty represents one standard deviation from the mean.
[13] W.-L. Wu, E. K. Lin, Q. Lin, and M. Angelopoulos, J. Appl. Phys. **88**, 7298 (2000).